Thin Solid Films 539 (2013) 245–250

Contents lists available at SciVerse ScienceDirect

Thin Solid Films

journal homepage: www.elsevier.com/locate/tsf

Study of the optical effects of nanostructure embedded GaN light emitting diodes formed by nanorod template overgrowth

Chi-Yu Wang [a,*], Yun-Chih Lee [b], Po-Shen Lee [b], Chia-Hao Chiu [b], Cheng-Huang Kuo [b], Mount-Learn Wu [b]

[a] Department of Electro-optical Engineering, Vanung University, Jhongli 32054, Taiwan, ROC
[b] Department of Optics and Photonics, National Central University, Jhongli 32054, Taiwan, ROC

ARTICLE INFO

Article history:
Received 6 July 2012
Received in revised form 18 April 2013
Accepted 19 April 2013
Available online 2 May 2013

Keywords:
Nanorod epitaxial lateral overgrowth
Finite difference time domain
Gallium nitride
Light emitting diodes
Light extraction

ABSTRACT

In this paper, we used the finite difference time domain method to study the optical effect of nanostructures produced by the nanorod epitaxial lateral overgrowth (NELO) process on the light extraction of GaN Light Emitting Diode (LED). It was found that these nanostructures produced by NELO served as buffer layers for reducing stress and dislocations, as well as photon blocking layers for reducing the light penetrating sapphire substrates. We studied the effect of the nanostructure shape and density distribution on the light extraction efficiency of GaN LED because various overgrowth conditions can lead to different shapes and distributions of nanostructures. Simulation results showed that curved surface nanopores and dual-sized nanorod structures formed during overgrowth on the nanorod template have an extraction efficiency that is almost 100% higher than that of conventional LEDs, and 30% higher than that of original nanorod embedded LEDs. This is because of the higher probability of photon reflection and the strong surface scattering from the curved surface of nanopores and extra air gap of dual-sized nanorod structures. It was also shown that the density of the nanostructure occupied area affects light extraction. The simulation analysis shows that the light intensity peaks coincide in the locations of the nanopore gathered region, indicating that photon reflection is enhanced by nanopores. Experiments also showed that the electro luminescence emission from LEDs with 12.5% nanostructure density is 30% stronger than that of conventional LED.

1. Introduction

GaN-based light-emitting diodes (LEDs) are becoming more appealing in applications ranging from vehicular indicator lights to solid-state lighting. This is due to their superior energy efficiency, high reliability, and versatile colors. However, when considering LED lighting as a replacement for fluorescent lighting, several characteristics such as brightness, compactness, and cost should be taken into account. The brightness of the LED is strongly related to the output efficiency of the LED chips and is the most important of these characteristics. Several approaches have been proposed and demonstrated with an aim to improve the output efficiency of GaN-based LED chips. Some of these are surface texturing [1–3], photonic crystals [4,5], nanoporous or nanorod GaN template by nanoepitaxial lateral overgrowth (NELO) processes [6–8], patterned sapphire substrates [9], thin GaN structures [10], and flip-chip packaging [11].

Of these approaches, several groups implemented nanoepitaxial lateral overgrowth (NELO) processes to improve the epi-growth quality in GaN LEDs [6–8], and these technologies are of particular interest since they exhibit superior device performance. The nanopatterned GaN substrate produced by NELO serves as a buffer layer that reduces the stress and dislocations [8,12]. It is generally considered that the enhanced light efficiency of LEDs having nanostructures is due to the improved internal quantum efficiency and material epitaxial quality. However, no evaluation has yet been proposed concerning the optical extraction mechanism in LEDs that have these nanostructures which are produced by the nanorod template overgrowth process. However, there is a lack of clarity on the optical extraction of nanoporous structures, e.g., the optical extraction mechanism for nanoporous LEDs is not yet realized.

In this paper, we propose optical properties for nanoporous GaN LEDs produced by GaN nanorod template overgrowth. We present the numerical analysis of the optical enhancement of nanostructure embedded GaN LEDs using the finite difference time domain (FDTD) method. The simulation results indicate that these nanopatterned templates that are produced by NELO serve as photon blocking layers that reduce the light penetrating the sapphire substrate. The analysis results also show that the shape and distribution of these nanostructures significantly affect the light extraction characteristics of LEDs. We obtained a 40% enhancement in the light extraction using nanostructure embedded GaN LEDs with a 12.5% filling factor by simulation. This is in agreement with the electroluminescence (EL) measurement data also shown in the report.

* Corresponding author.
E-mail address: chiyuwang@mail.vnu.edu.tw (C.-Y. Wang).

0040-6090/$ – see front matter
http://dx.doi.org/10.1016/j.tsf.2013.04.122

2. Experiments (device fabrication)

In our experiments, a 1.8-μm-thick undoped GaN was grown on c-face (0001) 2-inch sapphire substrates by metal–organic chemical vapor deposition. A 40-nm-thick SiO_2 film was then deposited on the GaN surface by plasma-enhanced chemical vapor deposition chemical vapor deposition, followed by the electron beam evaporator of a Ni metal film. After rapid thermal annealing at 800 °C for 2 min under ambient nitrogen, a Ni metal film containing self-assembled nanoscale Ni metal islands was produced; this film can be used as hard mask for dry etching process [13,14]. The sample was then etched down to the sapphire substrate using inductively coupled plasma to form the nanorods. The resulting overgrowth epi-layers of 2.5 μm n-GaN, Multiple Quantum Wells (MQW) and 0.3 μm p-GaN were grown on the random nanorod GaN template from the nanoporous thin film. Standard photolithography and dry etching are then used to form the nanoporous LEDs. In terms of fabrication of the LED device, the p-type layer was selectively etched to expose the n-type GaN layer using an inductively-coupled plasma etching system. An Indium tin oxide transparent conducting layer was then deposited on the surface of the p-GaN layer. This was followed by the deposition of a Ni/Au (50 nm/200 nm) layer to form a p-electrode. To form an n-electrode, a Ti/Al (50 nm/200 nm) layer was deposited on the n-GaN layer. Fig. 1 shows the room temperature EL spectra of the fabricated LEDs with 20 mA dc injection current, including a nanoporous LED and conventional LED. The EL peak position of both of these LEDs was 450 nm. The EL intensity of the nanoporous LED was 30% higher than that of the conventional LED. In addition to the improvement of the epi quality due to the NELO process found by some groups [6–8], from an optical point of view, such an observation is also attributed to better light extraction efficiency [15]. This improved light extraction efficiency is due to more effective reflection of high spatial frequency photons for nanostructure embedded LEDs, resulting in more opportunities for the escape of photons from the LED surface.

3. Simulation results and discussion

Based on the different nanostructure configurations formed during the nanorod coalescence overgrowth process in GaN-LED, the optical properties of various configurations are analyzed below. The distribution and density of the nanostructures are also considered. The FDTD analysis method is used to study the near field radiation patterns of the nanostructure embedded LEDs. Details of the simulated procedures can be found elsewhere [16,17]. In order to describe the random propagation of unpolarized photons that are trapped within or escaping from LEDs, multiple TE and TM-polarized point sources having a wavelength of 454 nm are arranged with an interval of 100 nm within the

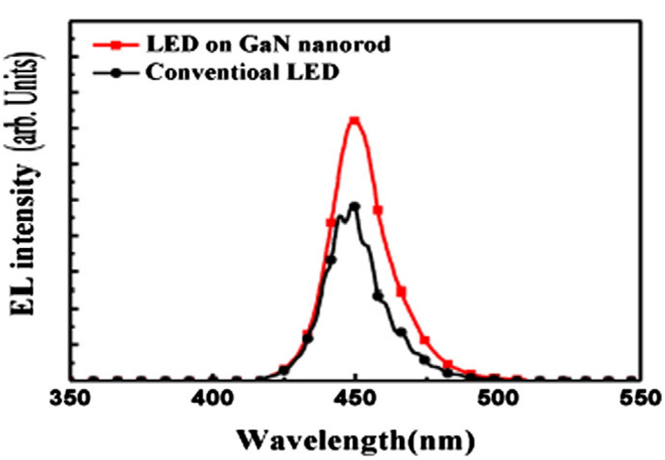

Fig. 1. Room temperature EL spectra of the nanoporous LED and conventional LED.

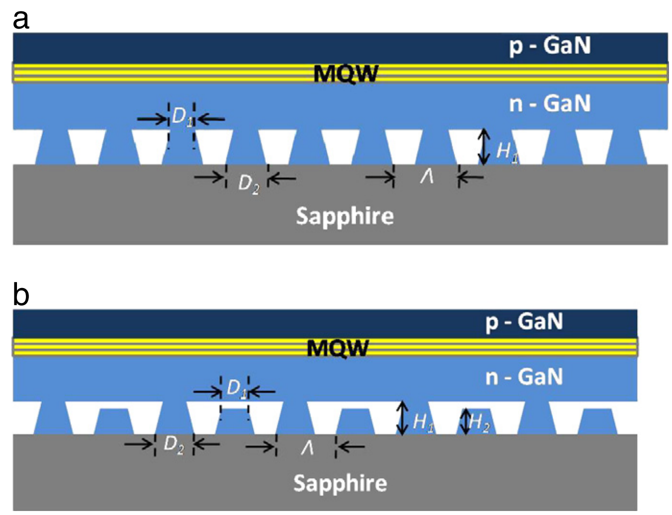

Fig. 2. The schematic diagrams of (a) a single-sized nanorod embedded GaN LED and (b) a dual-sized nanorod embedded GaN LED.

MQW region. For the convenience of analyzing the different configurations produced by the overgrowth conditions, several simplified and truncated schematics are adopted to simulate the nanostructure embedded LEDs.

3.1. Optical effect of nanorod-embedded GaN LEDs

In order to explain the effect of nanorod GaN templates on the improvement of the light extraction efficiency of LEDs, three different types of LEDs (a planar GaN template, a single-sized nanorod GaN template, and a dual-sized nanorod GaN template) are simulated, where the LEDs with the planar GaN template representing conventional GaN LEDs with no nanostructure. The schematic diagrams of the proposed LEDs with single-sized nanorod GaN templates and dual-sized nanorod GaN templates are shown in Fig. 2(a) and (b), respectively. The single-sized nanorod template is considered to be a nanostructure which maintains its perfect original nanorod shape during steps in the overgrowth process. The dual-sized case is considered to represent the voids that are produced by incomplete lateral growth over the neighboring nanorod, or defects that occur during the coalescence process shown in Fig. 3. The parameters of the structure for the single-sized nanorod GaN template include the period of the

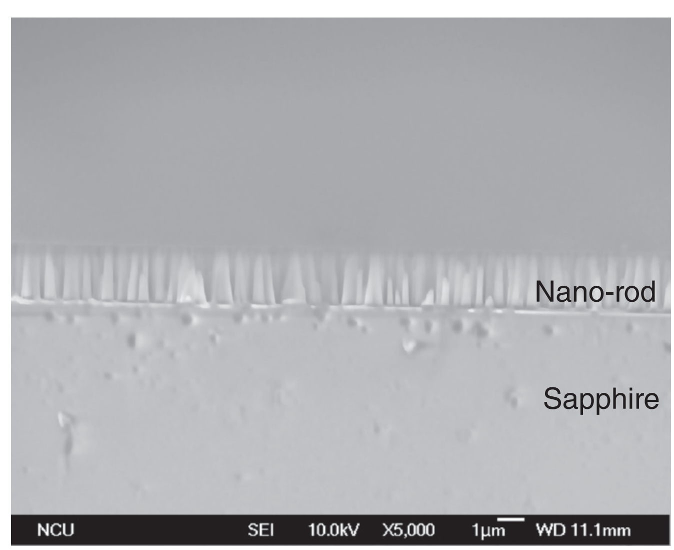

Fig. 3. The cross-sectional SEM picture of the nanorod GaN template.

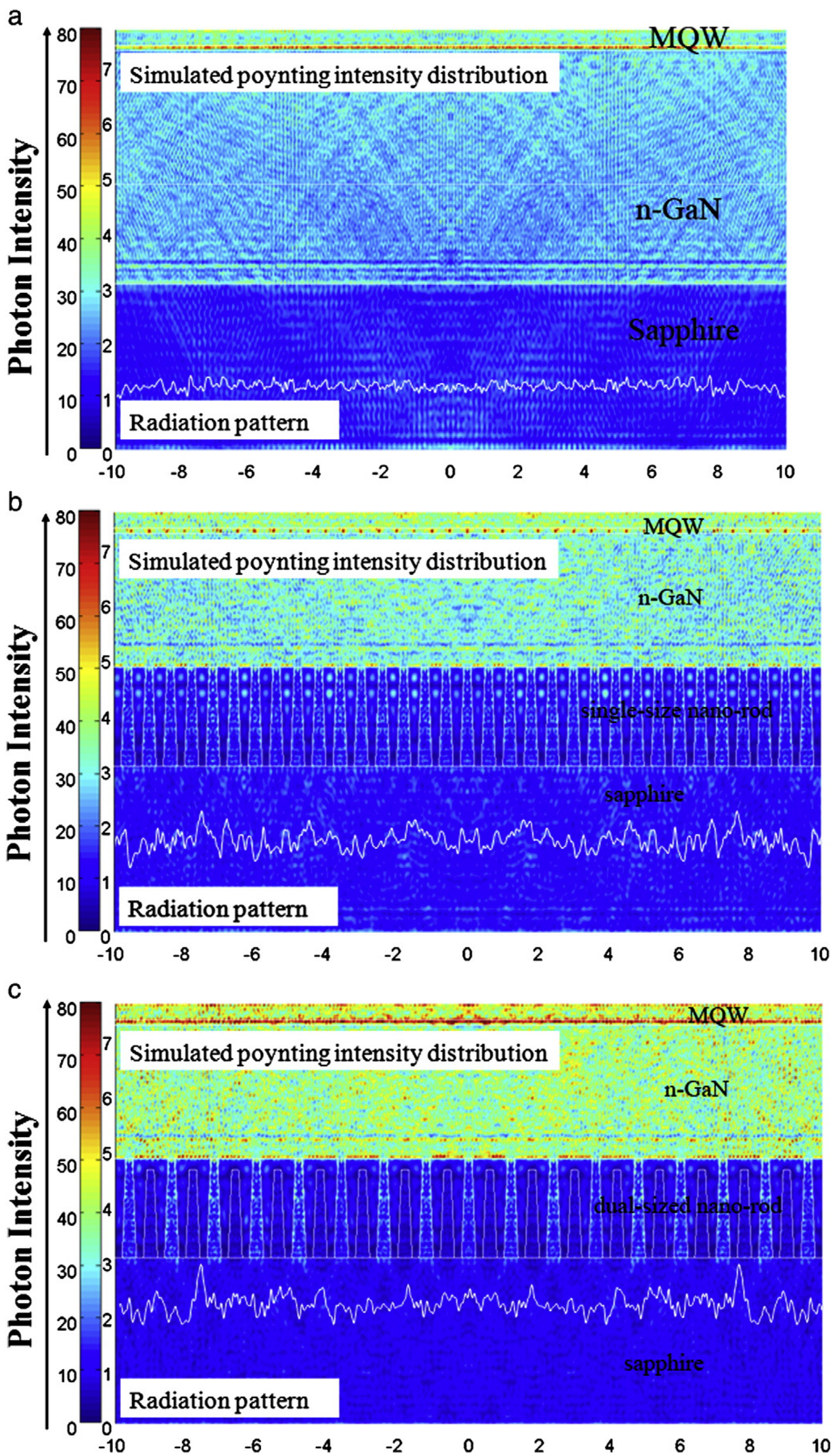

Fig. 4. Simulated Poynting-intensity distributions and the near-field confined intensity patterns for (a) LED I with a planar GaN template, (b) LED II with a single-sized nanorod GaN template, and (c) LED III with a dual-sized nanorod GaN template.

nanorod array $\Lambda = 0.6$ μm, filling factor of the nanorod $f = 0.5$, nanorod height $H_1 = 1.8$ μm, nanorod top diameter $D_1 = 0.2$ μm, nanorod bottom diameter $D_2 = 0.4$ μm, n-GaN layer thickness $H_{nGaN} = 4.3$ μm, MQW thickness $H_{MQWS} = 0.01$ μm, p-GaN layer thickness $H_{pGaN} = 0.3$ μm, p-GaN reflective index $n_{pGaN} = 2.5$, MQW reflective index $n_{MQWS} = 2.4$, and n-GaN reflective index $n_{nGaN} = 2.5$. The dual-sized nanorod GaN template illustrated in Fig. 2(b) is formed by combining two nanorods having heights $H_1 = 1.8$ μm and $H_2 = 1.6$ μm. As shown in Fig. 3, there are several defects on the template on which the epi-structure cannot be grown. The shorter nanorods that were added in Fig. 2(b) were applied to simulate the defects on the template with a regular arrangement defect density of 50%. The other structural parameters given in the numerical simulation are the same as those for the structure of LED grown on a single-sized nanorod GaN template.

Simulated pointing intensity distributions and radiation patterns are demonstrated in Fig. 4(a)–(c) for three different types of LEDs that have a planar GaN template (LED I), a single-sized nanorod GaN template (LED II), and a dual-sized nanorod GaN template (LED III). For comparison purposes, the simulated light emitted from LED I with the planar GaN template illustrated in Fig. 4(a) is applied as a base to study the effect of LEDs having different nanorod GaN templates (LEDs II and III). Fig. 4(b) shows the simulated light emission of LED II with a single-sized nanorod GaN template. In this simulation, the number of point sources of LED I is the same number that is arranged in the MQW region. When compared with the simulated results of LED I, the photon being emitted from the MQWs of LED II can be confined within the epi-layers between the single-sized nanorod GaN templates and air. This means that the single-sized nanorod GaN template prevents the penetration of photons into the sapphire substrate. Therefore, more photons can be coupled into the air from the top surface of the LED chip. This is the main cause of the improved light extraction of LED II when compared with that of LED I. By totally integrating the emitting power of LED II, the simulated enhancement factor of extracted light was 65.56% more than that for LED I.

Fig. 4(c) shows the simulation results for LED III obtained with a dual-sized nanorod GaN template. As illustrated in this figure, the photons emitted from the MQWs can also be confined within the epi-layers between the dual-sized nanorod GaN template and air. As shown in this figure, some photons are coupled into the sapphire substrate via the longer nanorods. However, a thin 0.2 μm layer of air between the epi-layer and the shorter nanorods (i.e., defects on the template), forms an isolation layer for the penetration of photons into the sapphire substrate. Therefore, when compared with LED II, more photons are reflected through the extra air gap that is produced by incomplete coalescence between the neighboring GaN nanorods. As a result of this extra air gap, light extraction was more than for the single-sized nanorod structure. By totally integrating the emitted power of LED III, the simulated enhancement factor of the extracted light was 96.53% more than that of LED I.

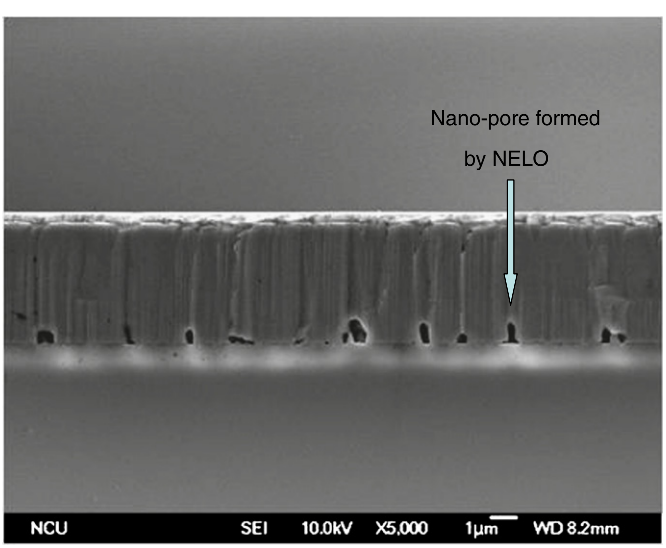

Fig. 5. Side view SEM picture of the nanorod GaN template after regrowth.

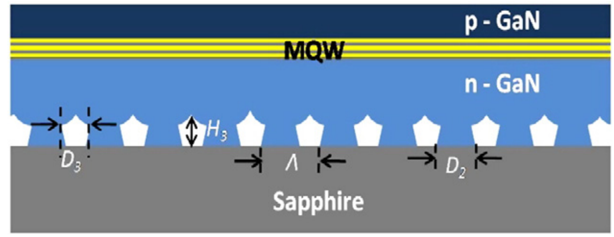

Fig. 6. The schematic diagram of the bent concave nanopore embedded GaN LEDs.

3.2. Optical effect of uniform nanopore-embedded GaN LEDs

Fig. 5 shows top side views of the scanning electron microscope (SEM) image of fabricated nanorod GaN templates. It is observed that some nanorods change shape during the coalescence overgrowth process in Fig. 5. In order to consider the light extraction due to this nanostructure configuration, simplified schematic diagrams of the bent concave nanopore embedded GaN LEDs are shown in Fig. 6. In the optical simulation of these proposed LEDs, we adopt two nanopores having different heights (H_3) of 1.8 and 0.8 μm, as well as bent concaves with a radius of 0.3 μm.

Fig. 7(a) shows the simulated light emission of LED IV with height $H_3 = 1.8$ μm for bent concave nanopore embedded LEDs. In this simulation, the same number of point sources is arranged in the MQW region as was the case for LED I. By totally integrating the emitting power of LED IV, the simulated enhancement factor of the extracted light is 89.66% more than that of LED I. As shown in this figure, due to its curved surface, a bent concave nanopore structure provides the light with a greater chance of being reflected and redirected. As a result, when compared with LED II, more light can escape to the air from the top surface of the LED via the curved top shape of this nanostructure. Fig. 7(b) shows the simulated light emission of LED V with a nanopore height of $H_3 = 0.8$ μm. In this simulation, the MQW region of LED V has the same number of point sources as was the case for LED I. By totally integrating the emitting power of LED V, the simulated enhancement factor of the extracted light extraction is 65.56% more than that of LED I. As seen in this figure, more photons in the GaN epi-layers can be coupled into the sapphire substrate via the shorter nanopores. Therefore, when compared with the case of LED IV which has longer nanopores, there is less enhancement in the extracted light.

3.3. Optical effect of the nanostructure distribution and density on LED light extraction

In our previous simulations, we studied the influence of the shape and size of nanostructures on the light extraction of LEDs, and a uniform nanostructure distribution with a density of 50% was adopted in the simulation. In this section, we discuss the optical effect of the distribution and density of nanostructures on LED light extraction. We arranged LED VI with 18 randomly distributed nanopores instead of the previously used 36 nanorods or uniform pore distribution. They were arranged on an LED device with length of 22 μm, and its schematic diagram is shown in Fig. 8. Fig. 9 shows the simulated light emission of this randomly distributed nanoporous LED VI with a 0.8 μm nanopore height and a 25% nanopore density. By totally integrating the emitting power of LED VI, the simulated enhancement factor of the extracted light is 58.55% higher than that of LED I. As shown in this figure, the lower density of the nanopores decreases the probability of light traveling towards the

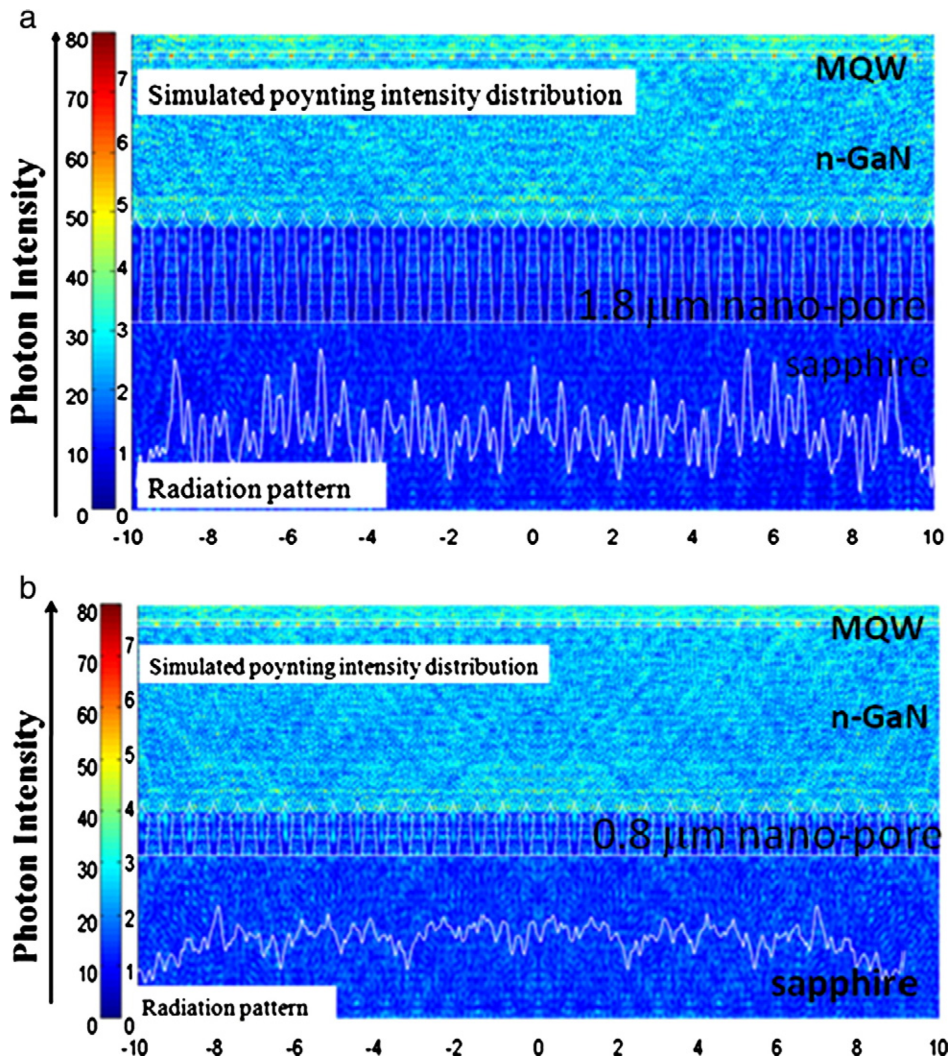

Fig. 7. Simulated Poynting-intensity distributions and the near-field confined intensity patterns for (a) LED IV with a nanopore height $H_3 = 1.8$ μm and (b) LED V with a nanopore height $H_3 = 0.8$ μm.

nanopore surface and the subsequent redirection that would cause light to escape from the LED surface. Based on the radiation pattern in Fig. 8, the light intensity peaks coincide at locations where there is a cluster of nanopores, and this indicates that photon reflection is induced by nanopores.

As shown in Fig. 5(a), our experimental results indicate that the nanopores are randomly distributed with a nanostructure density of about 12.5%. If the nanopore density reduces to 12.5%, the simulated enhancement factor of the extracted light becomes 40.13%. Due to the lower density of the nanopores, the photons in GaN epi-layers can be coupled to the sapphire substrate because of Fresnel's loss which occurred at the interface between the GaN template and the sapphire substrate. Photons are only reflected from the area occupied by the nanopores and can be coupled into the top surface of the LED chip.

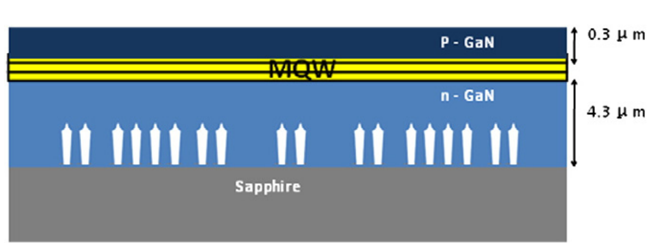

Fig. 8. The schematic diagram of the random distribution nanoporous LED VI with a nanopore height of 0.8 μm and a nanopore density of 25%.

The simulation results revealed that shape of the nanostructure plays an important role in photon behavior. Curved nanopore surfaces and an extra air gap for dual-sized nanorod structures that were formed during overgrowth on the nanorod template have a light extraction efficiency that is almost 100% higher than that for conventional LEDs, and almost 30% higher than for the original nanorod embedded LED. This is attributed to the higher probability that photons will be reflected, and the strong surface scattering that occurs due to the curved surface of nanopores and the extra air in dual-sized nanorod structures. The simulation results also demonstrate that the density of areas occupied by nanostructures plays an important role in the extraction of light. With respect to the radiation pattern simulated by nonuniform nanostructure embedded LEDs, the light intensity peaks appear mostly in the locations in which nanopores are present. This indicates that photon reflection is induced by nanopores, and that in the absence of these nanostructures, most of the light leaving the GaN/sapphire interface will not return to the GaN. Nanostructures in the LED, could provide more light scattering center than the micro-size structure, the light ray dynamics becomes chaotic, and allow more photons generated in the active layer to have multiple opportunities to find the escape cone, therefore, the nano sized structure could provide more light center than the micro size structure commonly used in the patterned sapphire substrate.

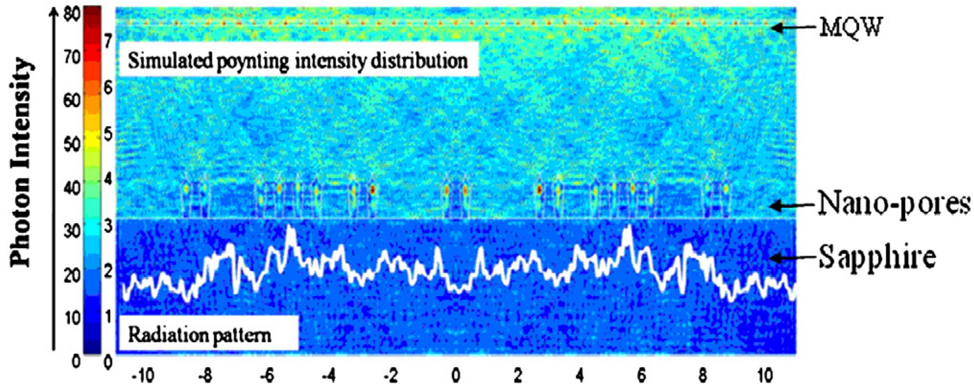

Fig. 9. Simulated Poynting-intensity distributions and the near-field confined intensity patterns for LED VI with a 0.8 μm nanopore height and a 25% nanopore density.

4. Conclusion

We studied the optical characteristics of the nanostructure embedded GaN LED that was produced by the NELO process using the FDTD method. Three configurations (single-sized nanorod, dual-sized nanorod, and bent concave nanopores) were adopted by simulating the different regrowth shapes of the NELO process. It was found that these nanostructures that were produced by NELO not only served as buffer layers that reduced the stress and dislocations, and also as photon blocking layers that reduced the amount of light penetrating through to the sapphire substrate. In the absence of these nanostructures, most of the light leaving the GaN/sapphire interface will not return to the GaN. The simulation results demonstrate that the shape and distribution of these nanostructures significantly affect the light extraction characteristics of LEDs. Enhancements in the extracted light are attributed to the escape of additional photons which is enabled by redirected light when reflected and scattered by these nanostructures. The nanostructures worked as reflectors which reflected the light initially emitted from the MQW layer toward the sapphire substrate. Therefore, the light has more opportunities to be redirected and escape through the semiconductor and air interface. The nanostructures studied in this paper included curved shape nanopores, dual nanorod structures, nanopores with higher air gaps, and nanostructures with higher densities or larger areas occupied by nanostructures. The light extraction significantly increased due to more opportunities for light to be reflected and redirected. The optical properties of the nanostructure embedded LED were also investigated by EL measurement. Based on our experimental conditions, the dominant EL emission from the nanostructure-embedded LED was 30% stronger than that for conventional LEDs. The EL results agree with the simulation prediction that the nanostructure embedded LED can provide a light extraction efficiency that is better than that of conventional LED samples.

References

[1] T. Fujii, Y. Gao, R. Sharma, E.L. Lu, S.P. DenBaars, S. Nakamura, Appl. Phys. Lett. 84 (2004) 855.
[2] T.N. Oder, K.H. Kim, J.Y. Lin, H.X. Jiang, Appl. Phys. Lett. 84 (1999) 466.
[3] C.H. Chan, C.H. Hou, S.Z. Tseng, T.J. Chen, H.T. Chien, F.L. Hsiao, Appl. Phys. Lett. 95 (2009) 011110.
[4] A. David, T. Fujii, R. Sharma, K. McGroddy, S. Nakamura, S.P. DenBaars, E.L. Hu, C. Weisbuch, H. Benisty, Appl. Phys. Lett. 88 (2006) 061124.
[5] C.H. Chao, S.L. Chung, T.L. Wu, Appl. Phys. Lett. 89 (2006) 091116.
[6] C.B. Soh, H. Hartono, S.Y. Chow, S.J. Chua, E.A. Fitzgerald, Appl. Phys. Lett. 90 (2007) 053112.
[7] Y.D. Wang, S.J. Chua, M.S. Sander, P. Chen, S. Tripathy, C.G. Fonstad, Appl. Phys. Lett. 85 (2004) 816.
[8] H.S. Chen, D.M. Yeh, Y.C. Lu, C.Y. Chen, C.F. Huang, T.Y. Tang, C.C. Yang, C.S. Wu, C.D. Chen, Nanotechnology 17 (2006) 1454.
[9] Z.H. Feng, Y.D. Qi, Z.D. Lu, Kei May Lau, J. Cryst. Growth 272 (2004) 327.
[10] S.C. Hsu, C.Y. Liu, Electrochem. Solid-State Lett. 9 (2006) G171.
[11] S.J. Chang, C.S. Chang, Y.K. Su, C.T. Lee, W.S. Chen, C.F. Shen, Y.P. Hsu, S.C. Shei, H.M. Lo, IEEE Trans. Adv. Packag. 28 (2005) 273.
[12] H. Hartono, C.B. Soh, S.J. Chua, E.A. Fitzgerald, J. Electrochem. Soc. 154 (2007) 1004.
[13] P.H. Chen, Chuan Chang Li, C.H. Tsai, Y.C. Lee, W.C. Lai, M.L. Wu, C.H. Kuo, J.K. Sheu, IEEE J. Quantum Electron. 46 (2010) 1066.
[14] C.H. Kuo, L.C. Chang, H.M. Chou, J. Electrochem. Soc. 158 (2011) H961.
[15] C.H. Kuo, L.C. Chang, H.M. Chou, IEEE Photon. Technol. Lett. 24 (2012) 608.
[16] M.L. Wu, Y.C. Lee, S.P. Yang, P.S. Lee, J.Y. Chang, Opt. Express 17 (2009) 6148.
[17] H.P. Shiao, C.Y. Wang, M.L. Wu, C.H. Chiu, IEEE Photon. Technol. Lett. 22 (2010) 1653.